BRAIN COMMUNICATIONS

Respiratory-related brain pulsations are increased in epilepsy—a two-centre functional MRI study

Janne Kananen,[1,2,3] Heta Helakari,[1,2,3] Vesa Korhonen,[1,2,3] Niko Huotari,[1,2,3] Matti Järvelä,[1,2,3] Lauri Raitamaa,[1,2,3] Ville Raatikainen,[1,2,3] Zalan Rajna,[1,4] Timo Tuovinen,[1,2,3] Maiken Nedergaard,[5,6] Julia Jacobs,[7,8,9,10] Pierre LeVan,[8,9,10,11,12] Hanna Ansakorpi[3,13,14] and Vesa Kiviniemi[1,2,3]

Resting-state functional MRI has shown potential for detecting changes in cerebral blood oxygen level-dependent signal in patients with epilepsy, even in the absence of epileptiform activity. Furthermore, it has been suggested that coefficient of variation mapping of fast functional MRI signal may provide a powerful tool for the identification of intrinsic brain pulsations in neurological diseases such as dementia, stroke and epilepsy. In this study, we used fast functional MRI sequence (magnetic resonance encephalography) to acquire ten whole-brain images per second. We used the functional MRI data to compare physiological brain pulsations between healthy controls ($n = 102$) and patients with epilepsy ($n = 33$) and furthermore to drug-naive seizure patients ($n = 9$). Analyses were performed by calculating coefficient of variation and spectral power in full band and filtered sub-bands. Brain pulsations in the respiratory-related frequency sub-band (0.11–0.51 Hz) were significantly ($P < 0.05$) increased in patients with epilepsy, with an increase in both signal variance and power. At the individual level, over 80% of medicated and drug-naive seizure patients exhibited areas of abnormal brain signal power that correlated well with the known clinical diagnosis, while none of the controls showed signs of abnormality with the same threshold. The differences were most apparent in the basal brain structures, respiratory centres of brain stem, midbrain and temporal lobes. Notably, full-band, very low frequency (0.01–0.1 Hz) and cardiovascular (0.8–1.76 Hz) brain pulses showed no differences between groups. This study extends and confirms our previous results of abnormal fast functional MRI signal variance in epilepsy patients. Only respiratory-related brain pulsations were clearly increased with no changes in either physiological cardiorespiratory rates or head motion between the subjects. The regional alterations in brain pulsations suggest that mechanisms driving the cerebrospinal fluid homeostasis may be altered in epilepsy. Magnetic resonance encephalography has both increased sensitivity and high specificity for detecting the increased brain pulsations, particularly in times when other tools for locating epileptogenic areas remain inconclusive.

1 Oulu Functional NeuroImaging (OFNI), Department of Diagnostic Radiology, Oulu University Hospital, Oulu 90029, Finland
2 Medical Imaging, Physics and Technology (MIPT), Faculty of Medicine, University of Oulu, Oulu 90220, Finland
3 Medical Research Center (MRC), Oulu 90220, Finland
4 Center for Machine Vision and Signal Analysis (CMVS), University of Oulu, Oulu 90014, Finland
5 Center for Translational Neuromedicine, Department of Neurosurgery, University of Rochester Medical Center, Rochester, NY 14642, USA
6 Center for Translational Neuromedicine, Faculty of Health and Medical Sciences, University of Copenhagen, Copenhagen 2200, Denmark
7 Department of Pediatric Neurology and Muscular Disease, University Medical Center Freiburg, Faculty of Medicine, University of Freiburg, Freiburg 79110, Germany
8 Department of Paediatrics, Cumming School of Medicine, University of Calgary, Calgary, AB T2N 4N1, Canada
9 Department of Neuroscience, Cumming School of Medicine, University of Calgary, Calgary, AB T2N 4N1, Canada

Received February 13, 2020. Revised April 29, 2020. Accepted May 5, 2020. Advance Access publication June 8, 2020

10 Hotchkiss Brain Institute and Alberta Children's Hospital Research Institute, University of Calgary, Calgary, AB T2N 4N1, Canada
11 Department of Radiology, Medical Physics, University Medical Center Freiburg, Faculty of Medicine, University of Freiburg, Freiburg 79110, Germany
12 Department of Radiology, Cumming School of Medicine, University of Calgary, Calgary, AB T2N 4N1, Canada
13 Research Unit of Neuroscience, Neurology, University of Oulu, Oulu 90220, Finland
14 Department of Neurology, Oulu University Hospital, Oulu 90029, Finland

Correspondence to: Vesa Kiviniemi, PhD, MD
Oulu Functional NeuroImaging (OFNI), Department of Diagnostic Radiology
Oulu University Hospital, P.O. Box 50, 90029 Oulu, Finland
E-mail: vesa.kiviniemi@oulu.fi

Correspondence may also be addressed to: Janne Kananen
E-mail: janne.kananen@oulu.fi

Keywords: brain physiology; brain pulsations; epilepsy; respiration; fast fMRI

Abbreviations: AED = antiepileptic drug; BBB = blood–brain barrier; BOLD = blood oxygen level dependent; CV = coefficient of variation; DN = drug-naive seizure patients; fMRI = functional MRI; HC = healthy control; MREG = magnetic resonance encephalography; PWE = patients with epilepsy; SP = spectral power; tSNR = temporal signal-to-noise ratio

Graphical Abstract

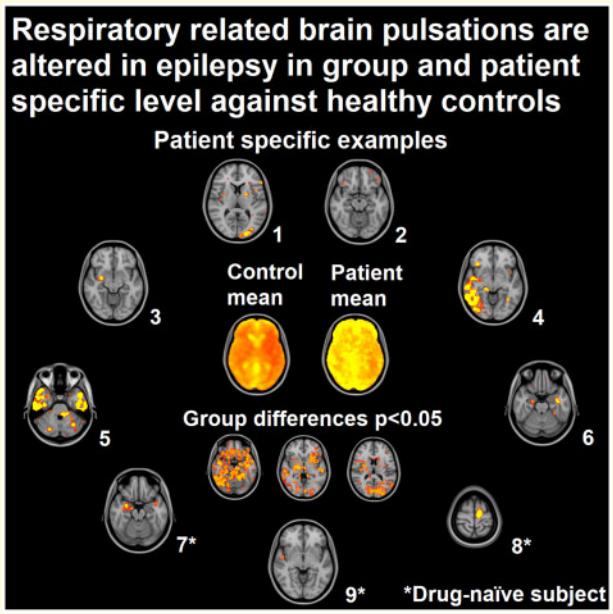

Introduction

Epilepsy is one of the most common neurological diseases and affects 50 million individuals worldwide annually (Fiest *et al.*, 2017). The most commonly used diagnostic tool in epilepsy is non-invasive scalp EEG, which can help to confirm the diagnosis and identify brain regions involved in the epileptic network (Smith, 2005; Tsiptsios *et al.*, 2010; Rosenow *et al.*, 2015). It is well established that hyperventilation induces epileptiform activity and thus is used as a provocation to increase the sensitivity of interictal EEG. In focal epilepsies, however, a positive EEG activation is obtained in only 6–30% of patients (Gabor and Marsan, 1969; Morgan and Scott, 1970; Guaranha *et al.*, 2005). The provocation of epileptic activity during hyperventilation results from a reduced pCO_2 and subsequently cerebral blood flow (Immink *et al.*, 2014).

The previous clinical evidence of respiration having a direct effect on epileptic activity has recently been supported by measurements of the effects of respiration on neuronal activity using intracranial electrodes. Respiration entrains electrophysiological brain rhythms in the mesiotemporal structures of patients with intractable epilepsy (Zelano *et al.*, 2016). Moreover, evidence has emerged that the cortical and limbic areas exhibit oscillations locked to the breathing cycle (Herrero *et al.*, 2018). In addition, it has been hypothesized that respiration not only supplies oxygen but also serves as a motor drive signal and a common clock that paces brain functions (Kleinfeld *et al.*, 2014).

Another non-invasive way of investigating neuronal activity in the brain is functional MRI (fMRI) utilizing T_2* (effective spin-spin) weighted blood oxygen level-dependent (BOLD) image contrast. The neurovascularly coupled BOLD signal changes have previously been analysed in people with epilepsy, to either map eloquent functional brain areas or identify networks involved in generating interictal and ictal epileptic activity (Chaudhary *et al.*, 2013; Constable *et al.*, 2013; Proulx *et al.*, 2014; Robinson *et al.*, 2017); e.g. language fMRI has been used in epilepsy surgical planning (Benjamin *et al.*, 2018). Resting-state fMRI studies aiming to identify epileptic activity have yielded several major findings. First, BOLD signal changes related to epileptic activity can be seen in all types of epilepsies and remain largely unaffected by brain pathologies (Laufs and Duncan, 2007; Gotman, 2008; van Graan *et al.*, 2015; Pittau *et al.*, 2017). Second, in patients in whom other diagnostic tools like interictal EEG, magnetoencephalography and PET remain inconclusive, fMRI might have additional value in localizing epileptic brain regions (Mankinen *et al.*, 2011, 2012; Wurina *et al.*, 2012; Constable *et al.*, 2013; Lee *et al.*, 2013; Sarikaya, 2015; Ergün *et al.*, 2016). Third, epileptic networks often extend beyond one focal epileptic generator and involve larger network structures including sub-cortical regions (Blumenfeld, 2014; Tracy and Doucet, 2015).

fMRI studies in epilepsy using conventional sequences often yield low sensitivity and have a limited ability to analyse the effect of physiological fluctuations in epileptic activity. A recent development in fast whole-brain fMRI sequences is so-called magnetic resonance encephalography (MREG), which allows fMRI measurement with higher temporal resolution (Lee *et al.*, 2013). In a direct comparison to standard fMRI, an increased sensitivity and both positive and negative BOLD effects were stronger in MREG within the epileptic focus identified in people with epilepsy (Jacobs *et al.*, 2014).

In addition to the haemodynamic BOLD effect to neuronal activity, fast fMRI sequences enable the detection of physiological oscillations as propagating cardiac and respiratory pulsations within their respective frequency subbands (Posse *et al.*, 2013; Kiviniemi *et al.*, 2016; Raitamaa *et al.*, 2019; Aslan *et al.*, 2019; Rajna *et al.*, 2019). Previously, these physiological pulsations have been regarded as artefacts with little relevance to the underlying pathology. However, these fluctuations are the driving forces of brain CSF pulsations and have been linked to several neurological diseases including epilepsy (Kananen *et al.*, 2018; Sun *et al.*, 2018; Rajna *et al.*, 2019). In particular, differences in the amplitude and variance in physiological BOLD signal fluctuations, as quantified by the coefficient of variation (CV), have been reported in different conditions, e.g. in acute ischaemic stroke (Khalil *et al.*, 2017), Alzheimer's disease (Makedonov *et al.*, 2016; Tuovinen *et al.*, 2017), small vessel disease (Makedonov *et al.*, 2013) and epilepsy (Kananen *et al.*, 2018). CV measures become more accurate when calculated over large distributions including thousands of samples and thus benefit from the high temporal resolution of MREG in the characterization of BOLD signal properties in frequency sub-bands of interest.

Our group published a preliminary study measuring physiological pulsations in patients with intractable epilepsy suggesting that pulsations were altered in patients compared to controls (Kananen *et al.*, 2018). In this study, we aim to replicate these findings in a larger group of patients, additionally introducing patient data with new onset epilepsy, thus allowing the exclusion of the effect of antiepileptic drugs (AEDs) as a cause of the observed change in brain pulsations. We hypothesize that brain pulsations measured with CV using fast fMRI differ between controls and patients both with chronic epilepsy and in drug-naive seizures.

Materials and methods

Participants

Patients with epilepsy (PWE), drug-naive seizure patients (DN) and healthy controls (HCs) were recruited to the study. The PWE group had focal epilepsy diagnosis of various aetiologies and AEDs. Majority of the PWE had intractable epilepsy and were under evaluation for surgery based on previous findings in the anatomical MRI. DN were imaged shortly after they had had a suspected epileptic seizure and with no earlier epilepsy diagnosis or AED. HC had no history of diagnosed neurological disorders.

Written informed consent was obtained from all participants according to the Declaration of Helsinki. The Ethics Committee of the Northern Ostrobothnia Hospital District, Finland, and Research Ethics Committee of the University of Freiburg, Germany, approved the research protocol.

Data acquisition

Subjects' fMRIs were obtained in Oulu and in Freiburg. The fMRI acquisition was performed using a three-dimensional single-shot stack of spirals sequence (MREG) that under-samples k-space to reach a sampling rate of 10 Hz (images per second), sufficient to image physiological pulsations (Assländer *et al.*, 2013). The point spread function of the stack of spirals sequence is 4.5 mm with minimized off-resonance effects compared to other k-space undersampling strategies like concentric shells and spokes (Zahneisen *et al.*, 2012; Assländer *et al.*, 2013). Imaging parameters are listed in Table 1. These specifications enabled imaging of the whole brain in 10 Hz with the voxel size of $3 \times 3 \times 3$ mm^3. The smaller slab thickness in Freiburg resulted in exclusion off the

Table 1 Scanning parameters in the different sites

	Oulu	Freiburg
Scanner	Siemens 3T SKYRA	Siemens 3T PRISMA
Coil	32-channel head coil	64-channel head-neck coil
Specifications for fMRI imaging (MREG)		
TR (ms)	100	100
TE (ms)	36	36
Flip angle (°)	25	25
3D matrix	64 × 64 × 64	64 × 64 × 50
Slab thickness (mm)	192	150

TE = echo time; TR = repetition time.

inferior parts of the brainstem in nine subjects divided equally between groups.

The resting-state fMRI data acquisition lasted up to 20 min. Due to scheduling reasons and/or subject compliance, some acquisitions had to be shortened to 5 min. To enable a consistent analysis, only the first 5 min from every dataset was used, similarly to previous work (Kananen *et al.*, 2018). Furthermore, the usage of the first 5 min minimized the vigilance drops of the subjects (Kiviniemi *et al.*, 2016; Kananen *et al.*, 2018). Study subjects wore earplugs to reduce noise and soft pads were fitted over the ears to minimize motion. During imaging, all participants received instructions to simply rest, stay awake and focus their gaze on a cross on a screen, which was shown via a mirror mounted on the head coil. High-resolution T_1-weighted anatomical reference images were obtained for co-registration of the MREG data to own anatomy and Montreal Neurological Institute space similarly to before (Kananen *et al.*, 2018).

Data preprocessing

MREG data were preprocessed with a standard Functional MRI of the Brain's software library pipeline and with the same procedures and steps as described in our previous papers (Kiviniemi *et al.*, 2016; Kananen *et al.*, 2018; Helakari *et al.*, 2019). The FIX ICA (Functional MRI of the Brain's independent component analysis-based Xnoiseifier) method was used for secondary artefact removal from the preprocessed MREG data (Griffanti *et al.*, 2014; Salimi-Khorshidi *et al.*, 2014). The FIX classifier was trained on previously collected control MREG data, imaged with identical parameters and was used identically for all subject groups.

Calculation methods

CV was used as a metric for the temporal variations in brain pulsations from the BOLD signal. Similar methods have been used in previous studies (Makedonov *et al.*, 2013, 2016; Jahanian *et al.*, 2014; Tuovinen *et al.*, 2017; Kananen *et al.*, 2018). For each preprocessed four-dimensional fMRI dataset, the CV values were calculated voxel-wise by CV= $[\sigma(X)]/[\mu(X)]$ where X is the time series of voxel, σ is the standard deviation and μ is the mean. Temporal signal-to-noise ratio (tSNR) is an established way to evaluate fMRI signal, and tSNR is calculated by tSNR = $[(\mu(X)]/[\sigma(X)]$, and thus tSNR = 1/CV. Here, in addition to voxel-wise CV, we calculated the brain-only single voxel tSNR values and after that individual whole head median tSNR (Griffanti *et al.*, 2014).

The CV maps, i.e. voxel-wise CV values, were calculated from full-band signal and three sub-bands: very low frequency 0.01–0.1 Hz, respiratory frequency 0.11–0.51 Hz and cardiovascular frequency 0.8–1.76 Hz by bandpassing full-band MREG signal. The respiratory and cardiac sub-bands were chosen based on the inspection of individual MREG signal frequency spectra, ensuring that the respiratory and cardiac peaks from all subjects were included within their respective sub-bands. Evaluated physiological mean cardiorespiratory frequencies were compared statistically between groups.

For the bandpassed CV calculation, the voxel-wise μ values were taken individually from unfiltered full-band signals. These full-band voxel-wise μ values were added to every timepoint of filtered signals for CV calculation in sub-bands, as the bandpass filtering operation demeans the signals. Sub-band CVs were calculated as described above. In addition, spectral power (SP) of sub-bands was calculated in sub-bands with statistically significant differences in the CV values between groups. Voxel-wise mean and standard deviation were calculated from HC group SP maps to convert all subjects' individual SP maps to Z-scores, yielding individual mappings of abnormal areas in epilepsy patients. For display purposes, all calculated maps were interpolated to 0.5 mm Montreal Neurological Institute space.

In addition, one cubic region-of-interest from the pneumotaxic and apneustic centres in the brainstem was chosen for signal calculation (Raitamaa *et al.*, 2019). Upper and lower smooth curves, i.e. envelopes outlining extremes for this signal, were calculated by finding the maximum and minimum peaks of the respiratory bandpassed signal and fitting a curve between peaks. These two curves were subtracted (max−min) from each other, to calculate the difference between envelopes, i.e. peak-to-peak amplitude, in any given timepoint. Mean values of amplitudes were compared statistically.

Functional MRI of the Brain's software library's motion correction data were used to inspect for between-group differences in the mean relative and absolute head motion.

All the procedures described were coded and calculated with MATLAB, Origin, Analysis of Functional NeuroImages and Functional MRI of the Brain's software library and are available upon request. Fine-tuning of images was performed with GNU Image Manipulation Program software.

Statistical analysis

The contrasts between the calculated map values of each group at each voxel were analysed with Functional

Magnetic Resonance Imaging of the Brain's software library's *randomise* with 50 000 Conditional Monte Carlo random permutations implementing family-wise error-corrected threshold-free cluster enhancement correction in both directions (HC > PWE/DN, HC < PWE/DN) separately (Smith and Nichols, 2009) with age, mean relative head motion and imaging site as a covariate. *T*-statistic maps with corrected *P*-values ($P < 0.05$) were created to evaluate statistically significant differences in the calculated average maps between the groups (Nichols and Holmes, 2002; Winkler *et al.*, 2014). In addition, differences between PWE and DN groups were analysed similarly. Statistical testing for the envelope and physiological cardiorespiratory rate differences between groups were performed using the unpaired two-way Student's *t*-test. Two-sample Kolmogorov–Smirnov test was used to evaluate difference between two histograms.

Data availability

The data that support the findings of this study are available from the corresponding author upon reasonable request.

Results

Subjects

The study sample consisted of 33 PWE (age 34.6 ± 10.2 years, 21 females, Table 2), 9 DN (age 34.3 ± 15.3 years, two females, Table 3) who were additionally analysed as a separate group and 102 HC (age 37.3 ± 15.4 years, 51 females). PWE were using 1–4 AEDs (c.f. Table 2). Seventeen PWE and 14 HC were recruited and imaged in the University Medical Center Freiburg. The remaining of the PWE ($n = 16$), DN ($n = 9$) and HC ($n = 88$) groups were recruited from the outpatient clinic at Oulu University Hospital or from different ongoing studies in the University of Oulu. All subjects were imaged between the years 2012 and 2019.

Group-level analysis

CV was significantly increased in the PWE compared to the HC when the fMRI signal was bandpass filtered to the respiratory frequency (CV_{resp}, Fig. 1A). The most prominent differences ($P < 0.05$) were located in the basal structures of the brain, upper brain stem respiratory pneumotaxic centre, midbrain and temporal lobes, including amygdalae, hippocampi, pallida and putamina. In addition, there are clusters of significant difference in visual cortex. Altogether, main areas affected are around cavernous sinus that drains the mediobasal and temporal brain structures including hippocampi and thalami.

No significant results were observed in the full band, cardiovascular (0.8–1.76 Hz) or very low frequency subbands (0.01–0.1 Hz). There were no significant increases in HC compared to PWE. Furthermore, there were no significant differences in any of the bands between neither HC and DN groups nor PWE and DN groups. In addition, median full-band tSNR values were compared with the control and patient groups, and there was a significant difference between the PWE and HC groups ($P = 0.031$, Supplementary Fig. 1). There were no other significant differences in tSNR values.

For a more thorough analysis, the SP within the respiratory sub-band (SP_{resp}) was calculated; significant increases in PWE sub-band power were even more prominent than in CV_{resp} (Fig. 1B). Between the statistical maps, similar areas were affected (correlation coefficient = 0.85, Fig. 1). A single mean map of SP_{resp} was calculated from HC and from PWE (Fig. 2A). A histogram plot of these maps in logarithmic scale is shown in Fig. 2B. These histograms show explicitly the significant difference in group mean ($P < 0.001$), while the distribution of values between groups remains alike (Fig. 2B).

In addition to the whole-brain analyses, a brainstem region-of-interest was analysed (Fig. 3A). In Fig. 3A, an example signal from one patient and one control is presented, and in Fig. 3B, amplitude difference is shown between these two examples. The difference between example subjects' respiratory frequencies did not explain the difference observed in later stages. The signal maximum and minimum smooth curves, i.e. envelopes were calculated, and the minimum envelope was subtracted from the maximum envelope to reveal envelope differences (Fig. 3C) and to calculate a mean over time. Statistical comparison of these mean values revealed a significant between-group difference (*P*-value = 0.0035, Fig. 3D).

Individual-level analysis

As the epileptogenic areas may reside anywhere in the brain, a more individual-level approach is preferable for a more precise interpretation. The individual voxel-wise *Z*-scoring, based on HC population ($n = 102$) mean and standard deviation values, presents an opportunity to characterize patients more accurately in the individual level. With Z-maps we were able to threshold CV differences over 10 SD from the HC mean, equalling *P*-value close to 0 in one- and two-tailed statistical analyses.

Twenty-five out of the 23 PWE had clusters of brain tissue over the *Z*-score >10 threshold. In contrast, none of the 102 controls exhibited any variation above this threshold. In Fig. 4A, six examples of these PWE subjects and their corresponding focal changes in SP_{resp} maps are presented. Moreover, the SP_{resp} values in some of the pathological pulsation clusters were very high. When the threshold was reduced to *Z*-score 6, i.e. 6 SD above normal mean, all but three of the PWE subjects showed areas of increased SP_{resp}. In 20 subjects of PWE (60%), the clusters correlated precisely with the known brain region affected (Fig. 4A, Table 2). Eight PWE had vivid clusters, but the correlation with the known region was less prominent.

Table 2 Clinical characteristics of recruited PWE

PWE	Age (years)	Sex	Duration from diagnosis	Diagnosis	MRI finding	AED
1	21	M	3 years	TLE R	MTS R	LEV, LCM
2	32	F	13 years	TLE R	Normal	LEV, LTG
3	23	F	18 years	TLE L	Normal	LCM, LEV
4	38	M	36 years	TLE L	FCD L T	OXC, LEV, ZNS
5	23	F	18 years	TLE R	FCD R insula	LTG
6	37	M	10 years	TLE bilateral	MTS bilateral	LTG, CBZ, PGB
7	45	F	14 years	TLE bilateral	EC T bilateral	OXC, LTG, PB
8	34	M	4 years	TLE R	Normal	TPR
9	22	F	6 years	TLE bilateral	MTS bilateral	BRV, LCM
10	59	M	38 years	TLE L	Cavernoma, FCD L T	LCM, CBZ
11	20	F	5 years	TLE R	Glioma R T	GBP, LCM
12	35	F	19 years	TLE R	Normal	LEV, PER
13	33	F	28 years	TLE bilateral	NF1 suspected	OXC, BRV
14	53	F	26 years	TLE R	Normal	OXC, LEV
15	29	M	9 years	TLE bilateral	MTS L	LCM, BRV
16	43	F	9 years	TLE bilateral	EC bilateral T	ZNS, BRV
17	27	M	26 years	FLE R	FCD F R	LTG, LEV, ZNS, PER
18	41	M	3 months	TLE L	Normal	OXC
19	40	M	4 months	TLE	Normal	OXC
20	32	M	8 years	TLE bilateral	Hippocampal oedema R	CBZ, PGB
21	38	F	10 years	TLE	HS R	LTG, TPR
22	26	F	19 years	FLE	Normal	CLB, LCM, LTG, VPA
23	52	F	4 years	TLE L	FCD L T	LCM, ZNS
24	36	M	6 years	TLE L	Arachnoid cyst	LEV, OXC, LCM
25	53	M	13 years	TLE R	DVA/Telangiectasia R	LTG, LCM, TPR
26	22	F	12 years	TLE R	FCD R T	VPA, LTG, CLB
27	25	F	11 years	TLE L	FCD L	OXC, ZNS
28	35	F	12 years	TLE R	Normal	TPR, LCM, CLB
29	26	F	7 years	TLE R	Arachnoid cyst RPituitary microadenoma RFCD R	LEV, LCM, LTG
30	39	F	16 years	TLE	Normal	LTG
31	35	F	17 years	TLE	Normal	PGB, ZNS
32	26	F	4 years	TLE R	Normal	LCM, TPR, BRV
33	43	F	4 years	TLE R	Normal	LTG

BRV = brivaracetam; CBZ = carbamazepine; CLB = clonazepam; DVA = developmental venous anomaly; EC = encephalocele; F = female; FCD = focal cortical dysplasia; FLE = frontal lobe epilepsy GBP = gabapentin; HS = hippocampal sclerosis; L = left; LCM = lacosamide; LEV = levetiracetam; LTG = lamotrigine; M = male; MTS = mesiotemporal sclerosis; NF1 = neurofibromatosis type 1; OXC = oxcarbamazebine; PB = phenobarbital; PER = perampanel; PGB = pregabalin; R = right; T = temporal; TLE = temporal lobe epilepsy; TPR = topiramate; VPA = valproic acid; ZNS = zonisamide.

Table 3 DN characteristics

DN	Age	Sex	Duration of symptoms	Diagnosis	MRI finding
1	16	M	4 years	TLE L	Normal
2	41	M	10 years	TLE L	Normal
3	39	M	1 year	TLE	Normal
4	18	M	9 months	JME, generalized	Normal
5	17	M	One seizure	No diagnosis	Normal
6	30	M	3 months	Focal epilepsy	Normal
7	39	F	No information	JME	Normal
8	60	F	One seizure	No diagnosis	DNET suspected
9	49	M	2 years	TLE	Temporal vascular degeneration L

DNET = dysembryoplastic neuroepithelial tumour; F = female; JME = juvenile myoclonus epilepsy; L = left; M = male; TLE = temporal lobe epilepsy.

When considering the DN population on an individual level, there were voxels in every patient with the same *Z*-score >10 as with the larger group of PWE subjects (Fig. 4B). Changes were similar between PWE and DN (Fig. 4). Affected areas were present, even though no diagnosis was set.

Motion and physiological frequencies

No significant differences between HC and all patients were observed in mean absolute (P-value = 0.456) or relative ($P = 0.076$) movement. Similarly, no significant differences were found in the cardiorespiratory frequencies

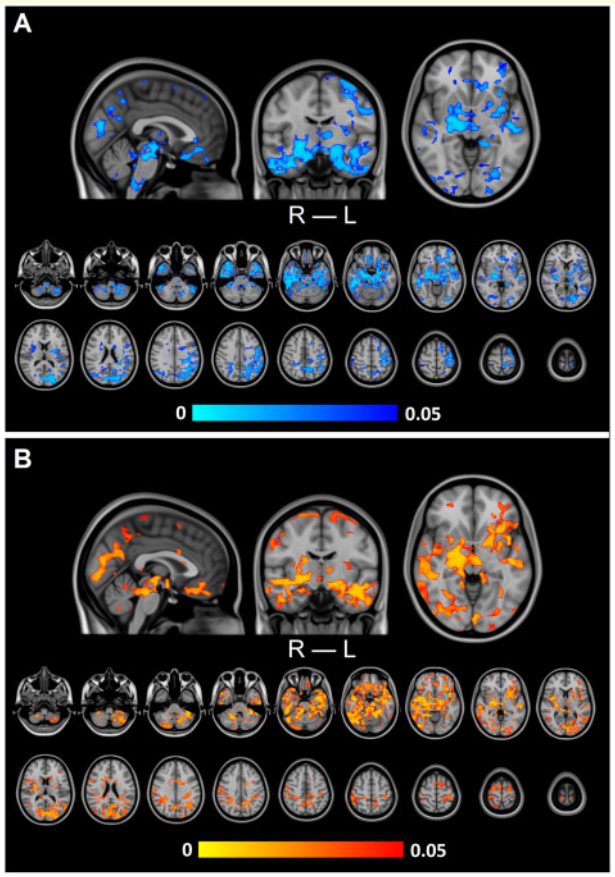

Figure 1 Group-level differences in respiration-related brain pulsation. (**A**) Variation in respiration-related brain pulsation (CV_{resp}) was significantly ($P < 0.05$) increased in PWE compared to HC. (**B**) Power of respiration-related brain pulsation (SP_{resp}) was significantly ($P < 0.05$) increased in PWE compared to HC. In both **A** and **B**, significant increases are located in basal structures of the brain, upper brain stems respiratory pneumotaxic centre, midbrain and temporal lobes, including also amygdalae, hippocampi, pallida and putamina.

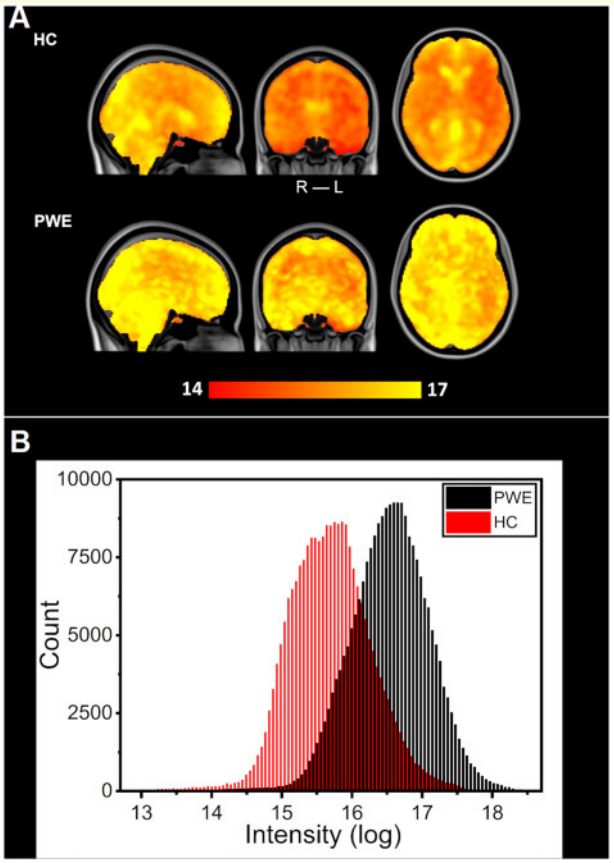

Figure 2 Mean spectral power of brain pulsations between HC and PWE groups. (**A**) Group mean maps in respiration-related power, transformed into a logarithmic scale. PWE group mean values are larger in the whole brain compared to HC. (**B**) Distributions of mean power in the respiratory sub-band voxel values in each group calculated from maps of section (**A**). Despite an overlap between the two similar distributions (HC: red, PWE: black), difference between the groups is highly significant ($P < 0.001$).

between groups (cardiac: HC mean = 65.9 ± 10.07 beats per minute, patient mean = 69.4 ± 10.19 beats per minute, $P = 0.068$; respiratory: HC mean = 15.0 ± 3.85 breaths per minute, patient mean = 16.3 ± 4.72 breaths per minute, $P = 0.100$). In HC, a mild bradycardia (<50 beats per minute) was present in three subjects.

Discussion

In this study, we analysed and provided evidence that respiratory-related T_2*-weighted fluctuations, i.e. brain pulsations are increased in epilepsy. Further analysis revealed that the power of these pulsations was much higher in patient-specific focal areas. The differences were not related to breathing-induced motion as no significant differences were observed in motion or in any of the physiological cardiorespiratory frequencies. These findings confirm our earlier preliminary results from a smaller sample size (Kananen *et al.*, 2018). Furthermore, we found that even without AED the pulsation abnormality is detected, since the individual DN subjects exhibited similar suprathreshold changes as the PWE. However, there were no significant group-level differences between the HC and DN groups. This may arise due to the smaller population and more heterogeneous composition of the DN group, which included both patients with generalized epilepsy syndrome and subjects with one confirmed seizure without epilepsy diagnosis.

Increased respiratory brain pulsations

In this study, we show that respiratory-related brain pulsations are different in PWE compared to HC. However, in contrast to our previous preliminary study (Kananen

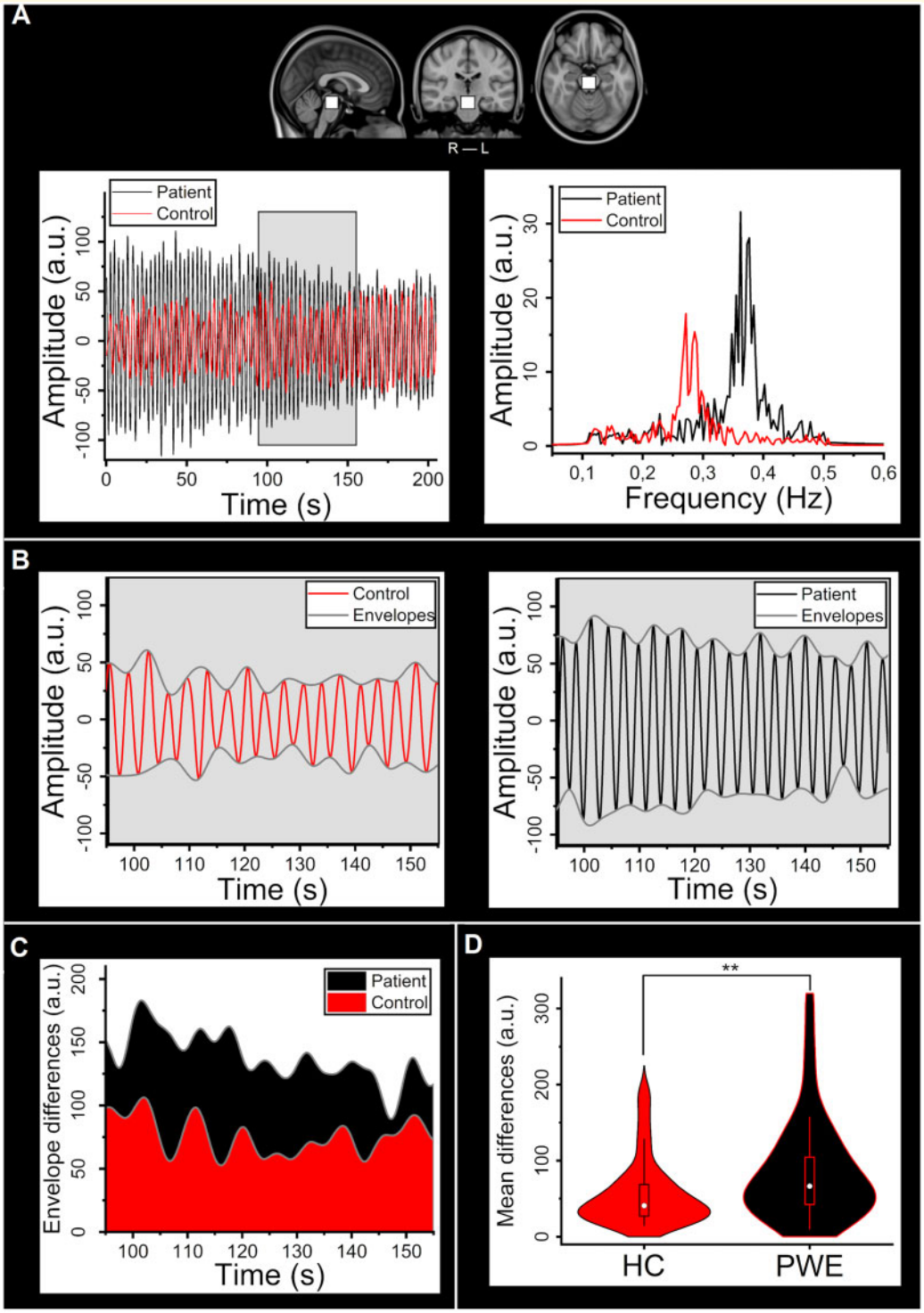

Figure 3 Differences in the respiratory bandpass filtered signal within the brainstem ROI. (**A**) The selected ROI in the upper brainstem area and example individual bandpass filtered signals from the PWE (black) and HC (red) groups and their respective frequency spectra. (**B**) Individual time-domain signals shown in **A** and corresponding individual lower and upper signal envelopes (control: red, patient: black). (**C**) Difference of envelopes (max−min) i.e. amplitude of signal for the example subjects (control: red, patient: black). (**D**) Violin plot of mean envelope differences between groups (HC: red, PWE: black). Groups differ significantly ($P = 0.0035$). ROI = region-of-interest.

et al., 2018), we observed no significant differences in other investigated frequency bands excluding respiratory sub-band. This may be due to more stringent use of covariates in the statistical testing. There was a significant difference in full-band median tSNR values between HC and PWE groups. Keeping in mind the previous results

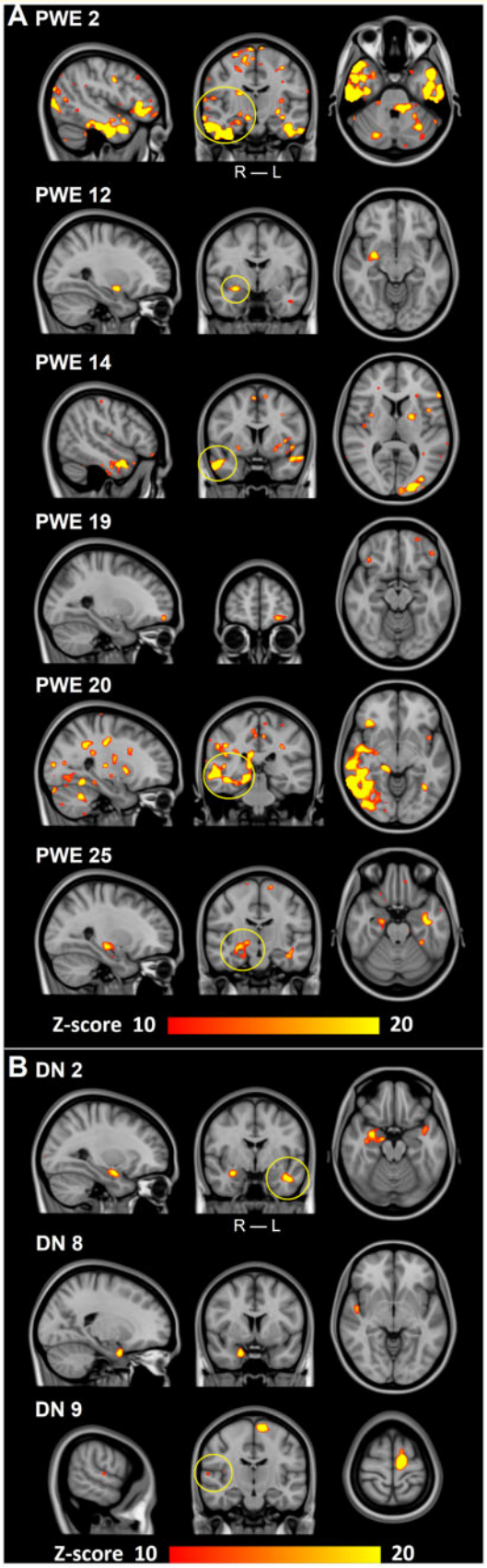

Figure 4 Individual changes in respiratory-related brain pulsations power. (**A**) Six examples of individual findings after thresholding (Z-score > 10) from PWE. All PWE show different areas of increased spectral power that correlate with the clinical diagnosis (yellow circles in coronal plane) in Table 2. PWE 19 has a TLE, although our method found affected areas in the frontal parts of the brain. First three PWE are from Freiburg and last three from Oulu. (**B**) Three DN examples of individual findings after thresholding (Z-score > 10). All DN have different areas influenced similarly as in **A** and which correlate with the known clinical diagnoses (yellow circles in coronal plane) in Table 3. DN 8 had a clear affected area, even though no diagnosis could be set with standard diagnostic tools. ROI = region-of-interest; TLE = temporal lobe epilepsy.

and the connection between tSNR and CV, the result was expected, especially because no covariates were used in median tSNR value analysis. Furthermore, tSNR results are well comparable to BOLD results reported by Griffanti *et al.* (2014).

Previously, other researchers have shown that respiration modulates electrical brain activity (Zelano *et al.*, 2016; Herrero *et al.*, 2018). They further postulated that the respiratory effects were applicable to the general population. However, they could only investigate intractable epilepsy patients due to the need for intracranial EEG recordings. Our results agree with the finding that respiration modulates brain pulsations (Zelano *et al.*, 2016; Herrero *et al.*, 2018).

Source of physiological pulsation signal

In the sense of brain MRI physics and brain physiology, the BOLD signal originates from transverse magnetization signal from coherent para/intravascular water proton spins. The spins' coherence and subsequently the BOLD signal increase as local paramagnetic deoxyhaemoglobin concentration reduces 3–5 s after neuronal activity triggers regional vasodilation (Silvennoinen *et al.*, 2003, Buxton, 2012, Kim and Ogawa, 2012). Envelopes of respiration rate and end tidal carbon dioxide are known to induce BOLD signal oscillations in the brain parenchyma overlapping but independent of underlying neuronally coupled haemodynamic activity (Wise *et al.*, 2004; Birn *et al.*, 2008).

It has been shown that the venous blood flow oscillations and the CSF flow pulsations are both driven by intrathoracic respiratory pressure changes (Dreha-Kulaczewski *et al.*, 2015, Vinje *et al.*, 2019). More precisely, one single inspirium induces venous outflow from the brain, that is counterbalanced by CSF inflow (Dreha-Kulaczewski *et al.*, 2017). The previously detected T_2* signal increase in brain parenchyma during inspiration is explained by reduced deoxyhaemoglobin in cortical veins and increased CSF in surrounding paravascular spaces (Kiviniemi *et al.*, 2016). The detected respiratory MRI signal in large CSF spaces that lacks (deoxy)haemoglobin

is flow related (Dreha-Kulaczewski *et al.*, 2015, 2017; Kiviniemi *et al.*, 2016; Huotari *et al.*, 2019).

In fast imaging, where repetition time $\ll T_1^*$ (apparent longitudinal relaxation time in the presence of inflow, 1.48 s) of the tissue (Kim and Ogawa, 2012), the MRI signal inflow effects need to be more thoroughly investigated. In addition, the physiological brain pulsations may induce local elastic brain fluctuation/motion that can be addressed with fast scanning more thoroughly in the future. Therefore, the interaction between the cardiac and respiratory pulsations in brain parenchyma is gathering increasing interest in fMRI (Chang *et al.*, 2013; Raitamaa *et al.*, 2019).

Pathophysiology behind differentiated pulsation

Our study revealed significant differences depicted by the elevated power of the PWE respiratory-related brain pulsations in amygdala, hippocampus, pallidum and putamen; brain structures known to be affected in multiple epilepsy types (Margerison and Corsellis, 1966; Hudson *et al.*, 1993; Pitkänen *et al.*, 1998; Aroniadou-Anderjaska *et al.*, 2008; Kandratavicius *et al.*, 2012; Kanner, 2012; Kanner *et al.*, 2012; Chatzikonstantinou, 2014; Wulsin *et al.*, 2016). Interestingly, these same areas are located around cavernous sinus, which is the main area of venous return canal of the mediobasal brain structures including the hippocampi and, additionally, an area where the CSF return pulses from the spinal canal re-enter the brain. In these areas, the respiratory tidal effects in perivenous space on MREG signal may be particularly strong.

The blood–brain barrier (BBB) is a neurovascular unit that insulates brain tissue interstitium from external ions in the blood and helps to maintain homeostasis for unhindered brain functionality. In epilepsy, the proper function of the BBB is altered, which results in abnormal function and seizures (van Vliet *et al.*, 2015; Rüber *et al.*, 2018). Furthermore, sleep affects epileptiform activity (Ellingson *et al.*, 1984; Binnie and Stefan, 1999; Méndez and Radtke, 2001; Klein *et al.*, 2003; Baldin *et al.*, 2017; Giorgi *et al.*, 2017) and BBB function (Jessen *et al.*, 2015; Cuddapah *et al.*, 2019). Moreover, evidence has emerged that improper function of the BBB may cause epilepsy altogether (Marchi *et al.*, 2016) and contribute to drug resistance in epilepsy (Liu *et al.*, 2012).

Furthermore, the outer edge of the BBB, namely the Aquaporin-4 concentrated astrocyte lining, has recently been described as an essential part of the glymphatic brain clearance system (Nedergaard, 2013). The glymphatic system is driven by cardiorespiratory brain pulsations that push CSF from the *limitans externa* of the BBB into the brain tissue and further drive soluble proteins into the perivascular space and away from the brain (Mestre *et al.*, 2018*b*). While some opposing views exist (Smith *et al.*, 2017; Abbott *et al.*, 2018; Faghih and Sharp, 2018), researchers have found increasing evidence of a pulsation-driven glymphatic system (Iliff and Nedergaard, 2013; Nedergaard, 2013; Xie *et al.*, 2013; Iliff *et al.*, 2015, Mestre *et al.*, 2018*a*, *b*; Rasmussen *et al.*, 2018; Lilius *et al.*, 2019; Mortensen *et al.*, 2019). Importantly, a recent human study using focused BBB opening demonstrated a supra-diffusive glymphatic convection of MRI contrast media from the brain parenchyma (Meng *et al.*, 2019). Fast MRI findings suggest that the respiration is a leading driving force of the CSF convection (Dreha-Kulaczewski *et al.*, 2015). Our group has discovered evidence that, on a macroscopic scale, the respiration may function as a driver of the glymphatic pulsations in the brain (Kiviniemi *et al.*, 2016; Kananen *et al.*, 2018; Raitamaa *et al.*, 2019; Huotari *et al.*, 2019). Taken together, the mounting evidence of perivascular Aquaporin-4 loss in the *limitans externa* along with the failure of the BBB suggests that a failure of the glymphatic CSF clearance could predispose brain tissue to epileptiform activity (Eid *et al.*, 2005, 2018; van Vliet *et al.*, 2015; Marchi *et al.*, 2016; Rüber *et al.*, 2018).

Individual local differences

Often only standard anatomical MRI is available for clinical decision-making, and it fails to detect abnormalities in 57% of the focal epileptogenic lesions (Von Oertzen *et al.*, 2002). PET findings are reported in 34–96% of epilepsy cases (Sarikaya, 2015). Non-invasive magnetoencephalography has limited value in identifying epileptic activity in deep-seated areas such as mesial temporal lobe. The method used in our study was able to detect highly significant (over 10 SD) focal changes in over 80% of the patients, while no changes were observed in any of the 102 controls. In our prior study, the CV_{resp} differences correlated well with described diagnostic findings and symptoms (Kananen *et al.*, 2018). In the current study, the areas affected, and areas of known clinical diagnoses were related in 60% of the PWE. In addition, emerging evidence points to epileptogenic areas that are distinct from, e.g. brain areas of epileptiformic activity usually viable for surgery in temporal lobe epilepsy (Wiebe *et al.*, 2001; Andrews *et al.*, 2019). Thus, these results indicate that our method could become a potential diagnostic tool in the future especially in situations where other methods yield no result and more focal findings are necessary.

Limitations of the study

In this study, all PWE subjects were diagnosed with focal epilepsy and majority had a diagnosis for temporal lobe epilepsy. Large group sizes and similar epilepsy type enhanced statistical power ensuring reliable results. Prior MRI studies have shown that some propagation pathways in the brain during seizures are similar in different focal epilepsies (Löscher and Ebert, 1996; Steriade, 2005;

Laufs *et al.*, 2011; Centeno and Carmichael, 2014). However, due to the great variety of aetiologies in epilepsy, a homogeneous patient population with matching diagnosis, involved brain area, AED and clinical characteristics is extremely difficult to assemble.

Siemens 3 T scanners were used in Oulu and Freiburg. However, scanners were of different models resulting in different scanner bore size and head coil. Therefore, the use of imaging site as a covariate in the analysis minimized potential confounding effects to ensure the reliability of the results. In addition, due to short acquisition, the slowest fluctuations appear only maximally three times, which may lead to less precise results in very low frequency band.

Future prospects

As the pneumotaxic centre was one of the main affected areas, and minding its physiological function, it would be of interest to analyse possible other differences in respiratory-related pulsations in the brain, e.g. pattern, timing or different effect of expirium/inspirium.

Earlier studies especially in mesial temporal sclerosis have shown absent aquaporin-4 channels in perivascular astrocytes. The absence of these channels may contribute to the observed pulsations in the brain. Therefore, it would be interesting to study the relationship between aquaporin-4 channels and the pulsations observed in fast fMRI more thoroughly.

Concerning diagnostic measures, even though our results are robust, a more thorough analysis is warranted. Cooperation with various clinics with adequate fast fMRI sequence is needed as it would greatly help in standardizing the analysis process and in determining the decision limits. In addition, simultaneous fast fMRI/EEG in conjunction with hyperventilation and even sleep deprivation analysis would yield more insight into the physiological background of our findings.

Conclusion

Our analysis revealed compelling and highly significant evidence for altered physiological signal variations, namely brain pulsations at the respiratory frequencies, in epilepsy. The observed changes were not explained by motion or physiological cardiorespiratory rates and are therefore most likely due to intrinsic brain pulsations. After calculating maps of SP and thresholding those maps based on control data, we identified highly focal increases in individual PWE and DN data further implying that the changes may be relevant as a diagnostic tool in epilepsy when focal findings are necessary, e.g. in focal treatments.

Supplementary material

Supplementary material is available at *Brain Communications* online.

Acknowledgements

We thank all the study subjects for participating in the study and all people who collected used datasets in both Finland and Germany. We also thank Jussi Kantola for computational administration and CSC—IT Center for Science Ltd. Finland for providing computational services.

Funding

This work was supported by grants from Finnish Academy (275352, 314497 to V.K.), Jane and Aatos Erkko Foundation (V.K.), KEVO grants from Oulu University Hospital (V.K.), The University of Oulu Scholarship Foundation (J.K.), Medical Research Center (MRC) -Oulu (J.K., H.H.), Maire Taponen Foundation (J.K.), Finnish Brain Foundation (J.K.), Instrumentarium Science Foundation (J.K.), Orion Research Foundation (T.T.), The Finnish Medical Foundation (T.T.) and DFG cluster BrainLinks-BrainTools EXC-1086 (P.L.).

Competing interests

The authors report no competing interests.

References

Abbott NJ, Pizzo ME, Preston JE, Janigro D, Thorne RG. The role of brain barriers in fluid movement in the CNS: is there a 'glymphatic' system? Acta Neuropathol 2018; 135: 387–407.

Andrews JP, Gummadavelli A, Farooque P, Bonito J, Arencibia C, Blumenfeld H, et al. Association of seizure spread with surgical failure in epilepsy. JAMA Neurol 2019; 76: 462–9.

Aroniadou-Anderjaska V, Fritsch B, Qashu F, Braga M. Pathology and pathophysiology of the amygdala in epileptogenesis and epilepsy. Epilepsy Res 2008; 78: 102–16.

Aslan S, Hocke L, Schwarz N, Frederick B. Extraction of the cardiac waveform from simultaneous multislice fMRI data using slice sorted averaging and a deep learning reconstruction filter. Neuroimage 2019; 198: 303–16.

Assländer J, Zahneisen B, Hugger T, Reisert M, Lee H-L, LeVan P, et al. Single shot whole brain imaging using spherical stack of spirals trajectories. Neuroimage 2013; 73: 59–70.

Baldin E, Hauser WA, Buchhalter JR, Hesdorffer DC, Ottman R. Utility of EEG activation procedures in epilepsy: a population-based study. J Clin Neurophysiol 2017; 34: 512–9.

Benjamin CFA, Li AX, Blumenfeld H, Constable RT, Alkawadri R, Bickel S, et al. Presurgical language fMRI: clinical practices and patient outcomes in epilepsy surgical planning. Hum Brain Mapp 2018; 39: 2777–85.

Binnie CD, Stefan H. Modern electroencephalography: its role in epilepsy management. Clin Neurophysiol 1999; 110: 1671–97.

Birn RM, Murphy K, Bandettini PA. The effect of respiration variations on independent component analysis results of resting state functional connectivity. Hum Brain Mapp 2008; 29: 740–50.

Blumenfeld H. What is a seizure network? Long-range network consequences of focal seizures. In: HE Scharfman, PS Buckmaster, editors. Issues in clinical epileptology: a view from the bench. Dordrecht: Springer Netherlands; 2014. p. 63–70.

Buxton RB. Dynamic models of BOLD contrast. Neuroimage 2012; 62: 953–61.
Centeno M, Carmichael DW. Network connectivity in epilepsy: resting state fMRI and EEG-fMRI contributions. Front Neurol 2014; 5: 93.
Chang C, Metzger CD, Glover GH, Duyn JH, Heinze H-J, Walter M. Association between heart rate variability and fluctuations in resting-state functional connectivity. Neuroimage 2013; 68: 93–104.
Chatzikonstantinou A. Epilepsy and the hippocampus. Front Neurol Neurosci 2014; 34: 121–42.
Chaudhary UJ, Duncan JS, Lemieux L. Mapping hemodynamic correlates of seizures using fMRI: a review. Hum Brain Mapp 2013; 34: 447–66.
Constable RT, Scheinost D, Finn ES, Shen X, Hampson M, Winstanley FS, et al. Potential use and challenges of functional connectivity mapping in intractable epilepsy. Front Neurol 2013; 4: 39.
Cuddapah VA, Zhang SL, Sehgal A. Regulation of the blood–brain barrier by circadian rhythms and sleep. Trends Neurosci 2019; 42: 500–10.
Dreha-Kulaczewski S, Joseph AA, Merboldt K-D, Ludwig H-C, Gartner J, Frahm J. Inspiration Is the Major regulator of human CSF flow. J Neurosci 2015; 35: 2485–91.
Dreha-Kulaczewski S, Joseph AA, Merboldt K-D, Ludwig H-C, Gärtner J, Frahm J. Identification of the upward movement of human CSF in vivo and its relation to the brain venous system. J Neurosci 2017; 37: 2395–402.
Eid T, Lee T-SW, Patrylo P, Zaveri HP. Astrocytes and glutamine synthetase in epileptogenesis. J Neurosci Res 2019; 97: 1345–62.
Eid T, Lee T-SW, Thomas MJ, Amiry-Moghaddam M, Bjornsen LP, Spencer DD, et al. Loss of perivascular aquaporin 4 may underlie deficient water and K+ homeostasis in the human epileptogenic hippocampus. Proc Natl Acad Sci USA 2005; 102: 1193–8.
Ellingson RJ, Wilken K, Bennett DR. Efficacy of sleep deprivation as an activation procedure in epilepsy patients. J Clin Neurophysiol 1984; 1: 83–101.
Ergün EL, Saygi S, Yalnizoglu D, Oguz KK, Erbas B. SPECT-PET in epilepsy and clinical approach in evaluation. Semin Nucl Med 2016; 46: 294–307.
Faghih MM, Sharp MK. Is bulk flow plausible in perivascular, paravascular and paravenous channels? Fluids Barriers CNS 2018; 15: 17.
Fiest KM, Sauro KM, Wiebe S, Patten SB, Kwon C-S, Dykeman J, et al. Prevalence and incidence of epilepsy A systematic review and meta-analysis of international studies. Neurology 2017; 88: 296–303.
Gabor AJ, Marsan CA. Co-existence of focal and bilateral diffuse paroxysmal discharges in epileptics. Clinical-electrographic study. Epilepsia 1969; 10: 453–72.
Giorgi FS, Maestri M, Guida M, Carnicelli L, Caciagli L, Ferri R, et al. Cyclic alternating pattern and interictal epileptiform discharges during morning sleep after sleep deprivation in temporal lobe epilepsy. Epilepsy Behav 2017; 73: 131–6.
Gotman J. Epileptic networks studied with EEG-fMRI. Epilepsia 2008; 49: 42–51.
van Graan LA, Lemieux L, Chaudhary UJ. Methods and utility of EEG-fMRI in epilepsy. Quant Imaging Med Surg 2015; 5: 300–12.
Griffanti L, Salimi-Khorshidi G, Beckmann CF, Auerbach EJ, Douaud G, Sexton CE, et al. ICA-based artefact removal and accelerated fMRI acquisition for improved resting state network imaging. Neuroimage 2014; 95: 232–47.
Guaranha MSB, Garzon E, Buchpiguel CA, Tazima S, Yacubian EMT, Sakamoto AC. Hyperventilation revisited: physiological effects and efficacy on focal seizure activation in the era of video-EEG monitoring. Epilepsia 2005; 46: 69–75.
Helakari H, Kananen J, Huotari N, Raitamaa L, Tuovinen T, Borchardt V, et al. Spectral entropy indicates electrophysiological and hemodynamic changes in drug-resistant epilepsy—a multimodal MREG study. Neuroimage Clin 2019; 22: 101763.
Herrero JL, Khuvis S, Yeagle E, Cerf M, Mehta AD. Breathing above the brain stem: volitional control and attentional modulation in humans. J Neurophysiol 2018; 119: 145–59.
Hudson LP, Munoz DG, Miller L, McLachlan RS, Girvin JP, Blume WT. Amygdaloid sclerosis in temporal lobe epilepsy. Ann Neurol 1993; 33: 622–31.
Huotari N, Raitamaa L, Helakari H, Kananen J, Raatikainen V, Rasila A, et al. Sampling rate effects on resting state fMRI metrics. Front Neurosci 2019; 13: 279. doi: 10.3389/fnins.2019.00279.
Iliff JJ, Goldman SA, Nedergaard M. Implications of the discovery of brain lymphatic pathways. Lancet Neurol 2015; 14: 977–9.
Iliff JJ, Nedergaard M. Is there a cerebral lymphatic system? Stroke 2013; 44: S93–5.
Immink RV, Pott FC, Secher NH, van Lieshout JJ. Hyperventilation, cerebral perfusion, and syncope. J Appl Physiol 2014; 116: 844–51.
Jacobs J, Stich J, Zahneisen B, Assländer J, Ramantani G, Schulze-Bonhage A, et al. Fast fMRI provides high statistical power in the analysis of epileptic networks. Neuroimage 2014; 88: 282–94.
Jahanian H, Ni WW, Christen T, Moseley ME, Tamura MK, Zaharchuk G. Spontaneous BOLD signal fluctuations in young healthy subjects and elderly patients with chronic kidney disease. PLoS One 2014; 9: e92539.
Jessen NA, Munk ASF, Lundgaard I, Nedergaard M. The glymphatic system: a beginner's guide. Neurochem Res 2015; 40: 2583–99.
Kananen J, Tuovinen T, Ansakorpi H, Rytky S, Helakari H, Huotari N, et al. Altered physiological brain variation in drug-resistant epilepsy. Brain Behav 2018; 8: e01090.
Kandratavicius L, Ruggiero RN, Hallak JE, Garcia-Cairasco N, Leite JP. Pathophysiology of mood disorders in temporal lobe epilepsy. Braz J Psychiatry 2012; 34: 233–45.
Kanner AM. Can neurobiological pathogenic mechanisms of depression facilitate the development of seizure disorders? Lancet Neurol 2012; 11: 1093–102.
Kanner AM, Schachter SC, Barry JJ, Hersdorffer DC, Mula M, Trimble M, et al. Depression and epilepsy: epidemiologic and neurobiologic perspectives that may explain their high comorbid occurrence. Epilepsy Behav 2012; 24: 156–68.
Khalil AA, Ostwaldt A-C, Nierhaus T, Ganeshan R, Audebert HJ, Villringer K, et al. Relationship between changes in the temporal dynamics of the blood-oxygen-level-dependent signal and hypoperfusion in acute ischemic stroke. Stroke 2017; 48: 925–31.
Kim S-G, Ogawa S. Biophysical and physiological origins of blood oxygenation level-dependent fMRI signals. J Cereb Blood Flow Metab 2012; 32: 1188–206.
Kiviniemi V, Wang X, Korhonen V, Keinanen T, Tuovinen T, Autio J, et al. A ultra-fast magnetic resonance encephalography of physiological brain activity—glymphatic pulsation mechanisms? J Cereb Blood Flow Metab 2016; 36: 1033–45.
Klein KM, Knake S, Hamer HM, Ziegler A, Oertel WH, Rosenow F. Sleep but not hyperventilation increases the sensitivity of the EEG in patients with temporal lobe epilepsy. Epilepsy Res 2003; 56: 43–9.
Kleinfeld D, Deschênes M, Wang F, Moore JD. More than a rhythm of life: breathing as a binder of orofacial sensation. Nat Neurosci 2014; 17: 647–51.
Laufs H, Duncan J. Electroencephalography/functional MRI in human epilepsy: what it currently can and cannot do. Curr Opin Neurol 2007; 20: 417–23.
Laufs H, Richardson MP, Salek-Haddadi A, Vollmar C, Duncan JS, Gale K, et al. Converging PET and fMRI evidence for a common area involved in human focal epilepsies. Neurology 2011; 77: 904–10.
Lee H-L, Zahneisen B, Hugger T, LeVan P, Hennig J. Tracking dynamic resting-state networks at higher frequencies using MR-encephalography. Neuroimage 2013; 65: 216–22.
Lilius TO, Blomqvist K, Hauglund NL, Liu G, Stæger FF, Bærentzen S, et al. Dexmedetomidine enhances glymphatic brain delivery of intrathecally administered drugs. J Control Release 2019; 304: 29–38.

Liu JYW, Thom M, Catarino CB, Martinian L, Figarella-Branger D, Bartolomei F, et al. Neuropathology of the blood–brain barrier and pharmaco-resistance in human epilepsy. Brain 2012; 135: 3115–33.

Löscher W, Ebert U. The role of the piriform cortex in kindling. Prog Neurobiol 1996; 50: 427–81.

Makedonov I, Black SE, MacIntosh BJ. BOLD fMRI in the white matter as a marker of aging and small vessel disease. PLoS One 2013; 8: e67652.

Makedonov I, Chen JJ, Masellis M, MacIntosh BJ. Physiological fluctuations in white matter are increased in Alzheimer's disease and correlate with neuroimaging and cognitive biomarkers. Neurobiol Aging 2016; 37: 12–8.

Mankinen K, Jalovaara P, Paakki J-J, Harila M, Rytky S, Tervonen O, et al. Connectivity disruptions in resting-state functional brain networks in children with temporal lobe epilepsy. Epilepsy Res 2012; 100: 168–78.

Mankinen K, Long X-Y, Paakki J-J, Harila M, Rytky S, Tervonen O, et al. Alterations in regional homogeneity of baseline brain activity in pediatric temporal lobe epilepsy. Brain Res 2011; 1373: 221–9.

Marchi N, Banjara M, Janigro D. Blood–brain barrier, bulk flow, and interstitial clearance in epilepsy. J Neurosci Methods 2016; 260: 118–24.

Margerison JH, Corsellis J. Epilepsy and temporal lobes: a clinical electroencephalographic and neuropathological study of the brain in epilepsy, with particular reference to temporal lobes. Brain 1966; 89: 499–530.

Méndez M, Radtke RA. Interactions between sleep and epilepsy. J Clin Neurophysiol 2001; 18: 106–27.

Meng Y, Abrahao A, Heyn CC, Bethune AJ, Huang Y, Pople CB, et al. Glymphatics visualization after focused ultrasound-induced blood–brain barrier opening in humans. Ann Neurol 2019; 86: 975–80.

Mestre H, Hablitz LM, Xavier AL, Feng W, Zou W, Pu T, et al. Aquaporin-4-dependent glymphatic solute transport in the rodent brain. eLife 2018a; 7: e40070.

Mestre H, Tithof J, Du T, Song W, Peng W, Sweeney AM, et al. Flow of cerebrospinal fluid is driven by arterial pulsations and is reduced in hypertension. Nat Commun 2018b; 9: 4878.

Morgan MH, Scott DF. EEG activation in epilepsies other than petit mal. Epilepsia 1970; 11: 255–61.

Mortensen KN, Sanggaard S, Mestre H, Lee H, Kostrikov S, Xavier ALR, et al. Impaired glymphatic transport in spontaneously hypertensive rats. J Neurosci 2019; 39: 6365–77.

Nedergaard M. Garbage truck of the brain. Science 2013; 340: 1529–30.

Nichols TE, Holmes AP. Nonparametric permutation tests for functional neuroimaging: a primer with examples. Hum Brain Mapp 2002; 15: 1–25.

Pitkänen A, Tuunanen J, Kälviäinen R, Partanen K, Salmenperä T. Amygdala damage in experimental and human temporal lobe epilepsy. Epilepsy Res 1998; 32: 233–53.

Pittau F, Ferri L, Fahoum F, Dubeau F, Gotman J. Contributions of EEG-fMRI to assessing the epileptogenicity of focal cortical dysplasia. Front Comput Neurosci 2017; 11:

Posse S, Ackley E, Mutihac R, Zhang T, Hummatov R, Akhtari M, et al. High-speed real-time resting-state FMRI using multi-slab echo-volumar imaging. Front Hum Neurosci 2013; 7: 479.

Proulx S, Safi-Harb M, LeVan P, An D, Watanabe S, Gotman J. Increased sensitivity of fast BOLD fMRI with a subject-specific hemodynamic response function and application to epilepsy. Neuroimage 2014; 93: 59–73.

Raitamaa L, Korhonen V, Huotari N, Raatikainen V, Hautaniemi T, Kananen J, et al. Breath hold effect on cardiovascular brain pulsations—a multimodal magnetic resonance encephalography study. J Cereb Blood Flow Metab 2019; 39: 2471–85.

Rajna Z, Raitamaa L, Tuovinen T, Heikkilä J, Kiviniemi V, Seppänen T. 3D multi-resolution optical flow analysis of cardiovascular pulse propagation in human brain. IEEE Trans Med Imaging 2019; 38: 2028–36.

Rasmussen MK, Mestre H, Nedergaard M. The glymphatic pathway in neurological disorders. Lancet Neurol 2018; 17: 1016–24.

Robinson LF, He X, Barnett P, Doucet GE, Sperling MR, Sharan A, et al. The temporal instability of resting state network connectivity in intractable epilepsy. Hum Brain Mapp 2017; 38: 528–40.

Rosenow F, Klein KM, Hamer HM. Non-invasive EEG evaluation in epilepsy diagnosis. Expert Rev Neurother 2015; 15: 425–44.

Rüber T, David B, Lüchters G, Nass RD, Friedman A, Surges R, et al. Evidence for peri-ictal blood–brain barrier dysfunction in patients with epilepsy. Brain 2018; 141: 2952–65.

Salimi-Khorshidi G, Douaud G, Beckmann CF, Glasser MF, Griffanti L, Smith SM. Automatic denoising of functional MM data: combining independent component analysis and hierarchical fusion of classifiers. Neuroimage 2014; 90: 449–68.

Sarikaya I. PET studies in epilepsy. Am J Nucl Med Mol Imaging 2015; 5: 416–30.

Silvennoinen MJ1, Clingman CS, Golay X, Kauppinen RA, van Zijl PC. Comparison of the dependence of blood R2 and R2* on oxygen saturation at 1.5 and 4.7 Tesla. Magn Reson Med 2003; 49: 47–60.

Smith S. EEG in the diagnosis, classification, and management of patients with epilepsy. J Neurol Neurosurg Psychiatry 2005; 76: ii2–7.

Smith SM, Nichols TE. Threshold-free cluster enhancement: addressing problems of smoothing, threshold dependence and localisation in cluster inference. Neuroimage 2009; 44: 83–98.

Smith AJ, Yao X, Dix JA, Jin B-J, Verkman AS. Test of the 'glymphatic' hypothesis demonstrates diffusive and aquaporin-4-independent solute transport in rodent brain parenchyma. Elife 2017; 6: e27679. doi: 10.7554/eLife.27679.

Steriade M. Sleep, epilepsy and thalamic reticular inhibitory neurons. Trends Neurosci 2005; 28: 317–24.

Sun B-L, Wang L, Yang T, Sun J, Mao L, Yang M, et al. Lymphatic drainage system of the brain: a novel target for intervention of neurological diseases. Prog Neurobiol 2018; 163-164: 118–43.

Tracy JI, Doucet GE. Resting-state functional connectivity in epilepsy: growing relevance for clinical decision making. Curr Opin Neurol 2015; 28: 158–65.

Tsiptsios DI, Howard RS, Koutroumanidis MA. Electroencephalographic assessment of patients with epileptic seizures. Expert Rev Neurother 2010; 10: 1869–86.

Tuovinen T, Rytty R, Moilanen V, Abou Elseoud A, Veijola J, Remes AM, et al. The effect of gray matter ICA and coefficient of variation mapping of BOLD data on the detection of functional connectivity changes in Alzheimer's disease and bvFTD. Front Hum Neurosci 2017; 10: 680.

van Vliet EA, Aronica E, Gorter JA. Blood–brain barrier dysfunction, seizures and epilepsy. Semin Cell Dev Biol 2015; 38: 26–34.

Vinje V, Ringstad G, Lindstrøm EK, Valnes LM, Rognes ME, Eide PK, et al. Respiratory influence on cerebrospinal fluid flow—a computational study based on long-term intracranial pressure measurements. Sci Rep 2019; 9: 9732.

Von Oertzen J, Urbach H, Jungbluth S, Kurthen M, Reuber M, Fernández G, et al. Standard magnetic resonance imaging is inadequate for patients with refractory focal epilepsy. J Neurol Neurosurg Psychiatry 2002; 73: 643–7.

Wiebe S, Blume WT, Girvin JP, Eliasziw M. A randomized, controlled trial of surgery for temporal-lobe epilepsy. N Engl J Med 2001; 345: 311–8.

Winkler AM, Ridgway GR, Webster MA, Smith SM, Nichols TE. Permutation inference for the general linear model. Neuroimage 2014; 92: 381–97.

Wise RG, Ide K, Poulin MJ, Tracey I. Resting fluctuations in arterial carbon dioxide induce significant low frequency variations in BOLD signal. Neuroimage 2004; 21: 1652–64.

Wulsin AC, Solomon MB, Privitera MD, Danzer SC, Herman JP. Hypothalamic-pituitary-adrenocortical axis dysfunction in epilepsy. Physiol Behav 2016; 166: 22–31.

Wurina Zang Y-F, Zhao S-G. Resting-state fMRI studies in epilepsy. Neurosci Bull 2012; 28: 449–55.

Xie L, Kang H, Xu Q, Chen MJ, Liao Y, Thiyagarajan M, et al. Sleep drives metabolite clearance from the adult brain. Science 2013; 342: 373–7.

Zahneisen B, Hugger T, Lee KJ, LeVan P, Reisert M, Lee H-L, et al. Single shot concentric shells trajectories for ultra fast fMRI. Magn Reson Med 2012; 68: 484–94.

Zelano C, Jiang H, Zhou G, Arora N, Schuele S, Rosenow J, et al. Nasal respiration entrains human limbic oscillations and modulates cognitive function. J Neurosci 2016; 36: 12448–67.